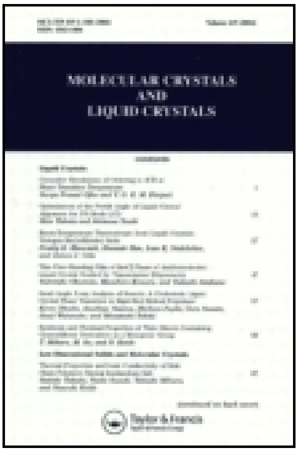

Molecular Crystals and Liquid Crystals
Publication details, including instructions for authors and subscription information:
http://www.tandfonline.com/loi/gmcl20

Comparison of Emission Characteristics with 4-, 5-, 6-Membered Iridium Complexes for OLEDs

Hye Rim Park [a] & Yunkyoung Ha [a]
[a] Department of Information Display Engineering, Hongik University, Seoul, 121-791, Korea

Version of record first published: 02 Aug 2012.

To cite this article: Hye Rim Park & Yunkyoung Ha (2012): Comparison of Emission Characteristics with 4-, 5-, 6-Membered Iridium Complexes for OLEDs, Molecular Crystals and Liquid Crystals, 563:1, 246-256

To link to this article: http://dx.doi.org/10.1080/15421406.2012.689729

Mol. Cryst. Liq. Cryst., Vol. 563: pp. 246–256, 2012
Copyright © Taylor & Francis Group, LLC
ISSN: 1542-1406 print/1563-5287 online
DOI: 10.1080/15421406.2012.689729

Comparison of Emission Characteristics with 4-, 5-, 6-Membered Iridium Complexes for OLEDs

HYE RIM PARK AND YUNKYOUNG HA*

Department of Information Display Engineering, Hongik University,
Seoul 121-791, Korea

To compare luminance efficiency, emission colors and stability of the iridium (III) complexes, we designed the four, five, six membered metallacycles of iridium with the various ancillary ligands. Picolinate as an ancillary ligand was known to form a stable five-membered metallacycle with the iridium center. In this study, 4-, 5-, and 6-membered metallacyclic iridium complexes chelated with acetanilide, (ace), picolinate (pic) and 8-quinolinecarboxylate (qc) were prepared, respectively, and their photophysical properties were investigated. As a main ligand, we introduced 2-phenylpyridine (ppy) and 2-(2,4-difluorophenyl)pyridine (F_2-ppy). The resulting Ir(ppy)$_2$(ace), Ir(ppy)$_2$(pic), Ir(ppy)$_2$(qc), Ir(F_2-ppy)$_2$(ace), Ir(F_2-ppy)$_2$(pic) and Ir(F_2-ppy)$_2$(qc) showed various emission maxima from 468 to 608 nm, depending upon the relative energy levels of their main and ancillary ligands. The emission preperties of the new iridium complexes revealed how the different ancillary ligands have influence on the luminous efficiency, emisson wavelength and stability of the iridium complexes, depending on the size of the metallacycle.

Keywords 4-, 5-, 6-membered ring; dopant material; iridium complexes; organic light-emitting diode (OLEDs); phosphorescence

Introduction

Phosphorescence-based organic light emitting diodes (OLEDs) have been actively developed in recent years. Use of the heavy transition metal complexes as emitting materials in OLEDs has an advantage with great emission efficiency, improved thermal stabilities [1]. Among the transition metal complexes, particularly, the iridium(III) complexes are known to have high efficiency and relatively short excited emissive states [2–4]. The phosphorescent iridium complexes have been used for OLEDs due to utilization of both singlet and triplet excited states for emission [5–7]. As a result, cyclometallated iridium complexes have attracted significant attention on account of their potential uses in various display material applications [8]. The very high quantum efficiency and the relatively short phosphorescence lifetime of the Ir complexes enable good performance in electrophosphorescence [9]. The Ir complexes with improved characteristics, in particular saturated phosphorescence color,

---

*Address correspondence Prof. Yunkyoung Ha, Department of Information Display Engineering, Hongik University, Sangsoo-dong, Mapo-gu, Seoul 121-791, Korea (ROK). Tel: (+82)2-320-1490; Fax: (+82)2-3142-0335. E-mail: ykha@hongik.ac.kr

high phosphorescence efficiency, and excellent physical properties have been widely studied [10,11]. Particularly, efficient phosphorescence color tuning is currently under active investigation with the aim of achieving full-color displays [12,13].

Previously, the cyclometallating main ligands were known to govern the emission color of the resulting complexes rather than the ancillary ligand. Recently, we have found that chemical modification of ancillary ligands enables tuning of the emitting properties of their complexes by the interligand energy transfer (ILET). Besides, the ancillary ligands for the iridium complexes tend to influence the perturbation degree of the metal-to-ligand charge transfer (MLCT) transition by the excited-state interaction with the cyclometallating ligand centered (LC) state, causing the minor change in emission wavelengths [14].

In general, most of the phosphorescent iridium complexes are formed five-membered metallacylic rings in which the chelating ligands are coordinated at the Ir center. In this work, we focused on the four, five, six membered metallacyclic iridium complexes and investigated luminous efficiencies, electrochemical characteristics and stability. The new iridium complexes, $Ir(ppy)_2(LX)$ and $Ir(F_2\text{-}ppy)_2(LX)$ (LX = acetanilide (ace), picolinate (pic) and 8-quinolinecarboxylate (qc)) were prepared and their luminescence properties were compared. We expected that the relative energy levels of the main ligands and ancillary ligands in the complexes could mostly determine luminescence characteristics of their iridium complexes. We wanted to investigate how the chemical structure of ancillary ligands in the complexes might influence the emission colors, luminance efficiencies and stability. We investigated the photoabsorption properties of the complexes with their UV-Vis spectra and studied the electrochemical characteristics with their cyclic voltammetric diagrams. The photoluminescence (PL) and electroluminescence (EL) of the complexes were also studied. The emitting colors and the device performances of the complexes, $Ir(ppy)_2(ace)$, $Ir(ppy)_2(pic)$, $Ir(ppy)_2(qc)$, $Ir(F_2\text{-}ppy)_2(ace)$, $Ir(F_2\text{-}ppy)_2(pic)$ and $Ir(F_2\text{-}ppy)_2(qc)$, were compared to find the involvement effect of the different ancillary ligands, ace, pic and qc, to the complexes.

Experimental

All reagents including 2-phenylpyridine (ppy) were purchased from Aldrich Co., except Ir(III) trichloride hydrate ($IrCl_3{\cdot}H_2O$), which was purchased from Strem Co., and used without further purification. All reactions were carried out under a nitrogen or argon atmosphere. Solvents were dried by standard procedures. Mass spectra were determined on JEOL, JMS-AX505WA, HP 5890 Series II Hewlett-Packard 5890A (capillary column) at Seoul National University in Korea.

Synthesis of Ligands and Iridium Complexes

Synthesis of F_2-ppy. 2,4-difluoro-2-phenylpyridine was obtained from the reaction of 2-chloropyridine and 2,4-difluorophenylboronic acid by Suzuki coupling [15]. Yield: 69%

Synthesis of $Ir(C\hat{}N)_2(ace)$.[$C\hat{}N$ = ppy, F_2-ppy] First, the cyclometallated Ir(III) μ-chloro-bridged dimer, $(C\hat{}N)_2Ir(\mu\text{—}Cl)_2Ir(C\hat{}N)_2$ (0.5 mmol), was prepared according to the Nonoyama method [16]. Second, the resulting dimer (0.107 g, 0.10 mmol) and acetylaniline (0.037 g, 0.25 mmol) were dissolved in dichloromethane (10 ml). Sodium methanolate (0.054 g, 1.0 mmol) was then added to the mixture, and stirred at room temperature for 24 h. The resulting precipitate was washed with water and diethyl ether, which further recrystallized in CH_2Cl_2/petroleum either [17].

[Ir(ppy)$_2$(ace)]: A yellow powder (Yield: 59%). FAB-MS: calculated 635; found 499 (M-ace).

[Ir(F$_2$–ppy)$_2$(ace)]: A yellow powder (Yield: 51%). FAB-MS: calculated 707; found 571 (M-ace).

Synthesis of Ir(C^N)$_2$(LX).[C^N = ppy, F$_2$-ppy, LX = pic, qc] First, the cyclometallated Ir(III) μ-chloro-bridged dimer, (C^N)$_2$Ir(μ—Cl)$_2$Ir(C^N)$_2$ (0.5 mmol), was prepared according to the Nonoyama method [16]. Second, the resulting dimer and LX were mixed in the solvent mixture of degassed CH_2Cl_2/EtOH/Et_3N (10 mL/10 ml/3 ml). The mixture was refluxed for 20 h at 80°C and the resulting precipitate was filtered after cooling and then washed with methanol [18].

[Ir(ppy)$_2$(pic)]: A yellow powder (Yield: 69%) [19].

[Ir(ppy)$_2$(qc)]: A yellow powder (Yield: 65%). FAB-MS: calculated 673; found 673. ^{1}H NMR (400 MHz, $CDCl_3$): δ 8.81–8.07 (d, 4H) 7.94–7.06 (m, 7H) 6.91–6.17 (m, 7H) 5.89 (d, 1H) 5.55 (d, 1H)

[Ir(F$_2$-ppy)$_2$(pic)]: A yellow powder (Yield: 55%) [20].

[Ir(F$_2$-ppy)$_2$(qc)]: A yellow powder (Yield: 67%). FAB-MS: calculated 745; found 746. ^{1}H NMR (400 MHz, $CDCl_3$): δ 9.10 (s, 2H) 8.31 (m, 4H) 7.80 (d, 1H) 7.75 (m, 3H) 7.40 (s, 1H) 7.23 (d, 1H) 7.17 (t, 1H) 6.77 (m, 1H) 6.46 (t, 1H) 6.38 (t, 1H) 5.68 (d, 1H) 5.58 (d, 1H).

Optical Measurements

UV-Vis absorption spectra were measured on a Hewlett Packard 8425A spectrometer. PL spectra were measured on a Perkin Elmer LS 50B spectrometer. UV-Vis and PL spectra of iridium complexes were measured in 10^{-5} M dilute CH_2Cl_2 solution.

Device Fabrication and Measurements

The OLEDs containing the heteroleptic iridium complexes as a dopant in emitting layers were fabricated. Glass substrate coated with a 180-nm-thick indium tin oxide (ITO) layer had a sheet resistance of 12 Ω/sq. All organic layers were sequentially deposited onto the substrate without breaking vacuum at a pressure of about 5×10^{-7} torr, using the thermal evaporation equipment. The organic materials were deposited as the following structure: 4,4′-bis[N-(naphthyl)-N-phenylamino]biphenyl (NPB, 50 nm) as hole transporting layer (HTL)/4,4′,4″-tris(N-carbazolyl)triphenylamine (TCTA, 10 nm) as buffer layer/iridium complex phosphors (10%) doped in 4,4′-bis(9-carbazolyl)-1,1′-biphenyl (CBP, 30 nm) as emitting layer/4,7-Diphenyl-1,10-phenanthroline (Bphen, 30 nm) as electron transporting layer (ETL)/lithium quinolate (Liq, 2 nm) as electron injection layer (EIL). The deposition rates were 1.0–1.1 and 0.1 Å/sec for organic materials and lithium quinolate (Liq), respectively. Finally, the aluminum cathode was deposited at a rate of 10 Å/sec. The devices were encapsulated in a glove box with O_2 and H_2O at concentrations below 1 ppm. The devices had emission areas of 3 × 3 mm^2. The electrical characteristics of devices and the EL spectra were measured and immediately recorded with a Chroma meter CS-1000A (Minolta). The current and voltage were controlled with a measurement unit (model 236, Keithely).

Results and Discussion

For the tuning of the emission color, there are some strategies involving the substituent effect or the control of the π conjugation length. In this study, on the other hand, we focused on the four, five, six membered metallacycles in the iridium center and compared their emission properties, luminance efficiency and stability in the device.

The synthesis of the iridium complexes, $Ir(C^\wedge N)_2(LX)$, ($C^\wedge N$ = ppy, F_2-ppy; LX = ace, pic, qc) were straightforward. The heteroleptic complexes, $Ir(ppy)_2(ace)$, $Ir(ppy)_2(pic)$, $Ir(ppy)_2(qc)$, $Ir(F_2\text{-}ppy)_2(ace)$, $Ir(F_2\text{-}ppy)_2(pic)$ and $Ir(F_2\text{-}ppy)_2(qc)$, were prepared according to the reported procedures [17–20]. The reaction schemes are illustrated in Fig. 1.

The UV-Vis absorption spectra of ppy and F_2-ppy series as the main ligands were compared, as shown in Fig. 2. The absorption spectra of these complexes have intense bands appearing in the ultraviolet part of the spectrum between 225 and 280 nm. These bands have been assigned to the spin-allowed $^1(\pi \rightarrow \pi^*)$ transitions of the ligands. The $^1(\pi \rightarrow \pi^*)$ bands are accompanied by weaker and lower energy features extending from 350 to 455 nm that have been assigned to both allowed and spin-forbidden MLCT transitions. The absorption peaks of $Ir(ppy)_2(LX)$ (LX = ace, pic, qc) around 225~350 nm were assigned to a spin-allowed metal charge transfer (^{1}MLCT) band, and the weaker absorption bands at the longer wavelengths can be attributed to the spin-forbidden ^{3}MLCT and spin-orbit coupling enhanced $^3\pi$-π^* transition. The absorption patterns of $Ir(ppy)_2(LX)$ (LX = ace, pic) and $Ir(F_2\text{-}ppy)_2(LX)$ (LX = ace, pic) are similar with absorption maxima at 261/405 nm, 264/401 nm 253/384 and 257/380 nm, respectively, while the complexes containing qc as a ancillary ligand showed absorption at the longer wavelength in the UV-Vis spectra.

The photoluminescence (PL) spectra of the iridium complexes prepared in this study were shown in Fig. 3. The emission wavelength of $Ir(ppy)_2(ace)$, $Ir(ppy)_2(pic)$, $Ir(ppy)_2(qc)$, $Ir(F_2\text{-}ppy)_2(ace)$, $Ir(F_2\text{-}ppy)_2(pic)$ and $Ir(F_2\text{-}ppy)_2(qc)$ appeared at 551, 504, 608, 523, 468 and 564 nm, respectively. The emission maxima of the iridium complexes were substantially shifted to the longer wavelength upon changing the main ligand from F_2-ppy to ppy,

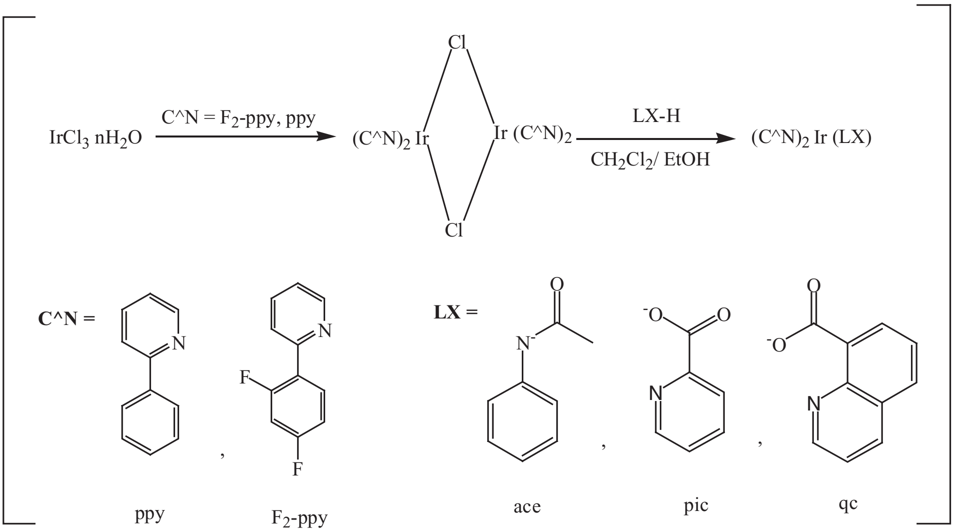

Figure 1. The synthesis of four, five and six-membered ring of $Ir(C^\wedge N)_2(LX)$, and their iridium complexes.

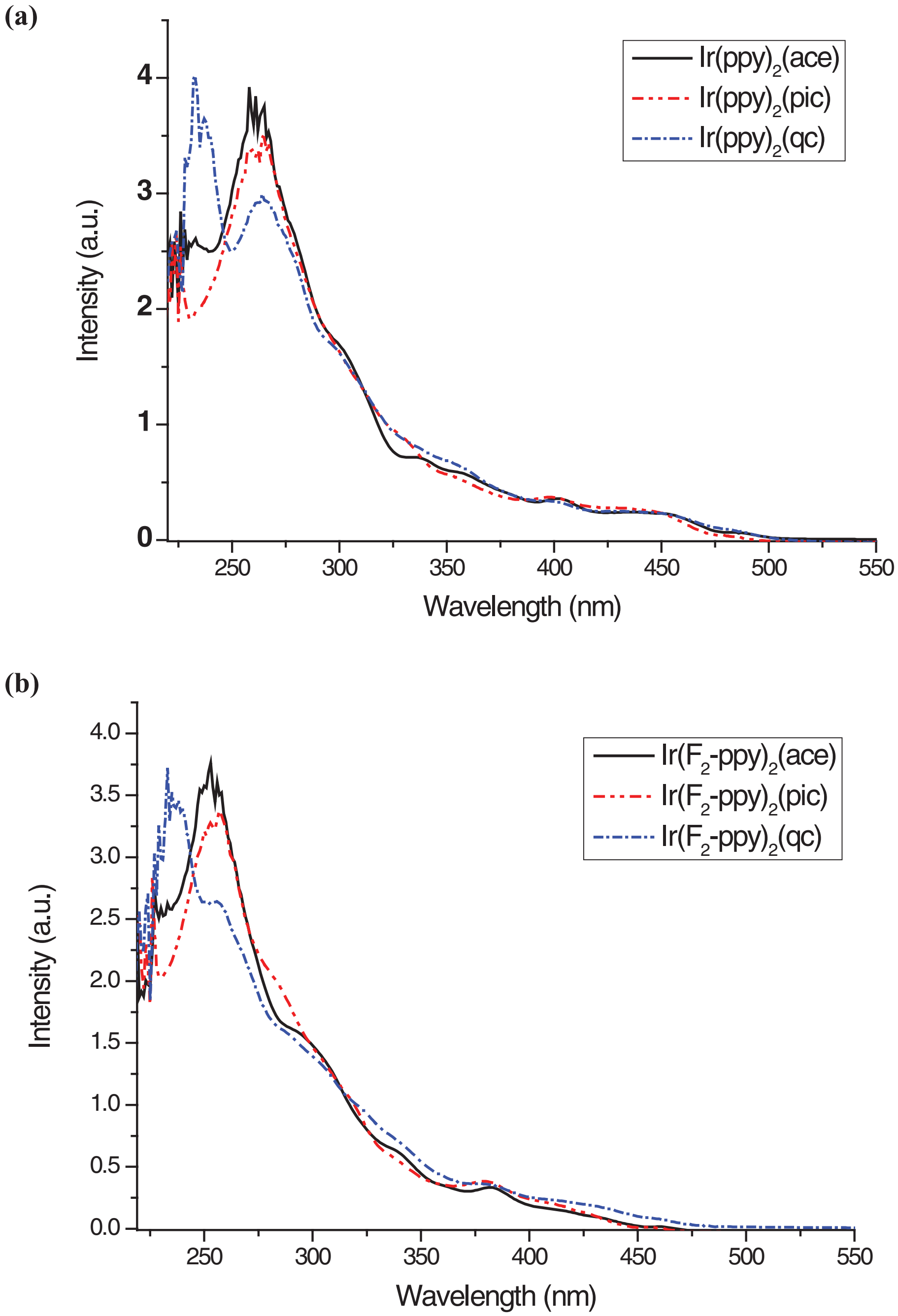

Figure 2. The UV-Vis absorption spectra of the heteroleptic iridium complexes of Ir(C^N)$_2$(LX) in a 10^{-5} M CH_2Cl_2 solution.

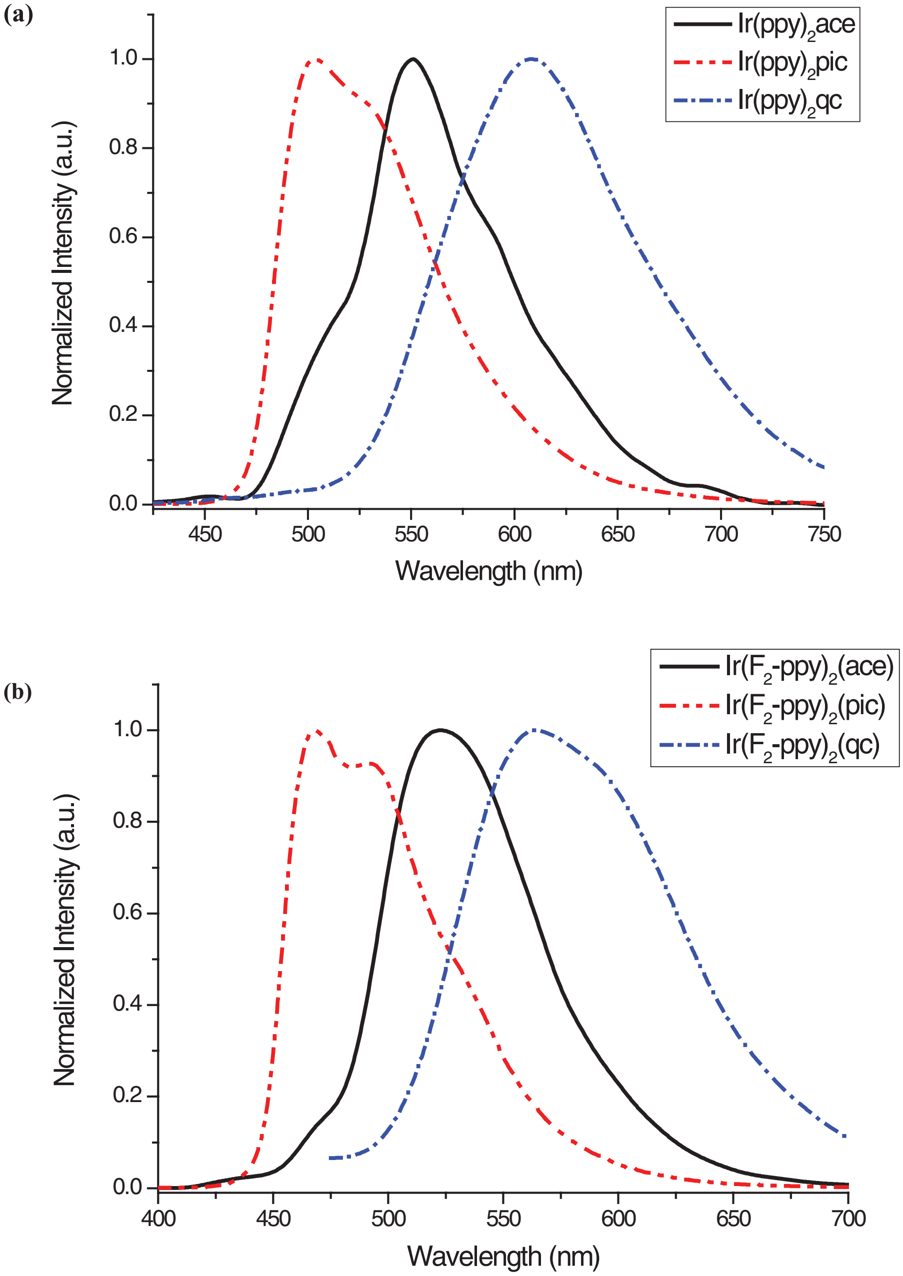

Figure 3. The PL spectra of Ir(ppy)$_2$(LX) (a) and Ir(F$_2$-ppy)$_2$(LX) (b) in a 10^{-5} M CH_2Cl_2 solution.

as expected. Interestingly, their emission maxima were substantially shifted to the longer wavelength upon the change of the ancillary ligand from ace to qc. The emission maxima of Ir(ppy)$_2$(ace) and Ir(ppy)$_2$(pic) were overlapped around 490 nm. Ir(C^N)$_2$(qc) has also a distinct feature of extremely broad emission band around 550–700 nm. The luminescence maxima of Ir(C^N)$_2$(qc) underwent the red shift presumably due to the extended

π conjugation length of qc ligand in the complexes. These results also support that qc ligand leads its iridium complexes to a different emission mechanism from those of iridium complexes, probably ILET.

We investigated electrochemical properties of the Ir complexes with the cyclic voltammetry (CV) as shown in Table 1, which could reveal their positions of the HOMOs and LUMOs [21,22]. The oxidation potential which indicates the HOMO of Ir(ppy)$_2$(ace), Ir(ppy)$_2$(ace) and Ir(ppy)$_2$(ace) were reversible at 0.31 and 0.58 V relative to an internal ferrocenium/ferrocene reference (Fc$^+$/Fc), respectively. The LUMOs of the complexes were estimated from their respective absorption spectra and electrochemical data, using the optical edge and band gap equation ($\Delta E = E_{ox} - E_{red}$). Their estimated reduction potentials were −2.60, −2.56 and −2.55 eV for Ir(ppy)$_2$(ace), Ir(ppy)$_2$(ace) and Ir(ppy)$_2$(ace), respectively. The detailed CV data of the heteroleptic iridium complexes were summarized in Table 1.

The electroluminescence (EL) properties of the complexes were also investigated for their OLED application. The configuration of the EL devices with Ir(F$_2$-ppy)$_2$(LX) and Ir(ppy)$_2$(LX) used as a dopant was ITO/NPB/TCTA/CBP:DOPANT (10%)/Bphen/Liq/Al. The EL peaks of devices with Ir(ppy)$_2$(ace), Ir(ppy)$_2$(pic), Ir(ppy)$_2$(qc), Ir(F$_2$-ppy)$_2$(pic) and Ir(F$_2$-ppy)$_2$(qc) were observed at 536, 513, 592, 461 and 559 nm, respectively, as shown

Table 1. Physical parameters for the iridium complexes

Ir complex	λ_{abs}/nm[a]	λ_{em}/nm[a]	E_{ox}/V[b]	HOMO/eV[c]	LUMO/eV[d]	ΔE/eV[d]
Ir(ppy)$_2$(ace)	258, 337, 402, 454	551	0.53	−5.33	−2.60	2.73
Ir(ppy)$_2$(pic)	264, 399, 448	504	0.58	−5.38	−2.56	2.82
Ir(ppy)$_2$(qc)	232, 356,401, 450	608	0.31	−5.11	−2.55	2.56
Ir(F$_2$-ppy)$_2$(ace)	253, 339, 384, 433	523	—	—	—	—
Ir(F$_2$-ppy)$_2$(pic)	257, 380, 418	468	—	—	—	—
Ir(F$_2$-ppy)$_2$(qc)	238, 255, 382, 457	564	—	—	—	—

Ir complex	molar extinction coefficient
Ir(ppy)$_2$(ace)	$3.92*10^4$, $0.71*10^4$, $0.36*10^4$, $0.22*10^4$
Ir(ppy)$_2$(pic)	$3.50*10^4$, $0.37*10^4$, $0.24*10^4$
Ir(ppy)$_2$(qc)	$3.99*10^4$, $0.64*10^4$, $0.33*10^4$, $0.23*10^4$
Ir(F$_2$-ppy)$_2$(ace)	$3.76*10^4$, $0.63*10^4$, $0.33*10^4$, $0.10*10^4$
Ir(F$_2$-ppy)$_2$(pic)	$3.38*10^4$, $0.38*10^4$, $0.17*10^4$
Ir(F$_2$-ppy)$_2$(qc)	$3.46*10^4$, $2.64*10^4$, $0.36*10^4$, $0.11*10^4$

[a]Measured in CH_2Cl_2 solution. [b]scan rate: 100 mV/s, Electrolyte: tetrabutylammonium hexafluorophosphate. The potentials are quoted against the internal ferrocene standard. [c]Deduced from the equation HOMO $= -4.8 - E_{ox}$, LUMO $= -4.8 - E_{red.}$ [d,e]Calculated from the optical edge and the relation $\Delta E =$ HOMO − LUMO.

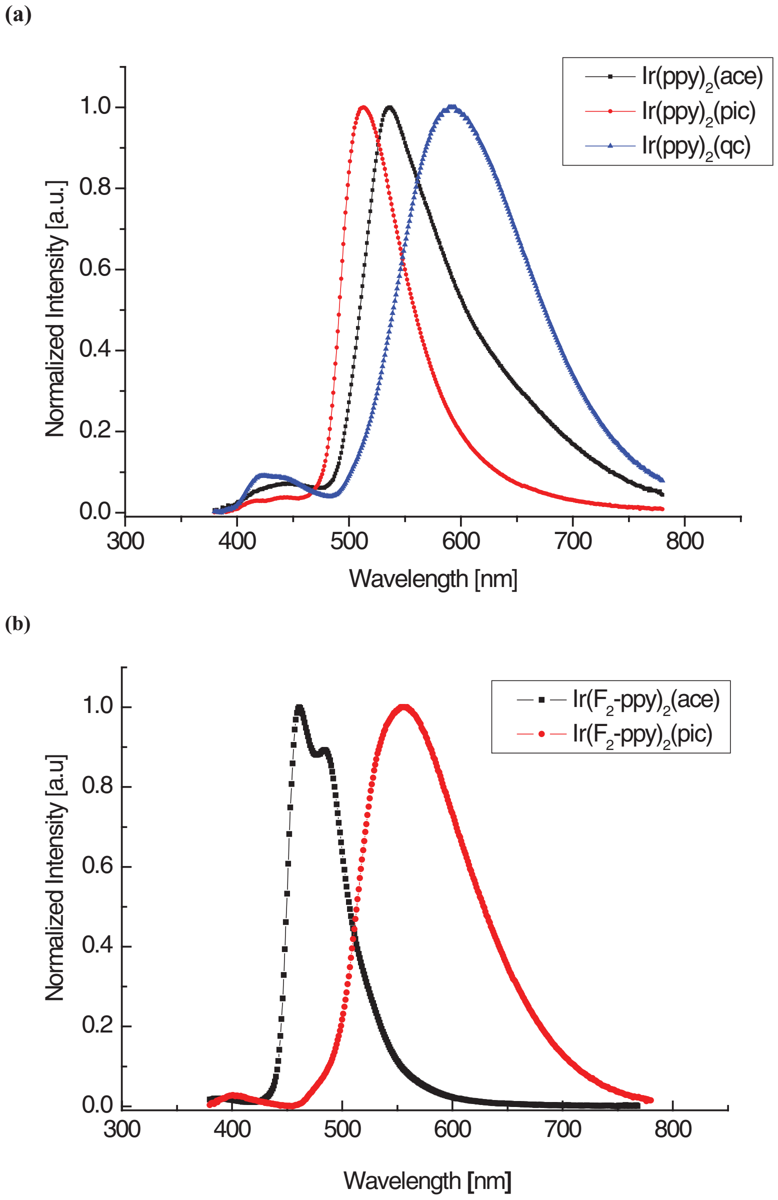

Figure 4. The EL spectra of the heteroleptic iridium complexes of Ir(C^N)$_2$(LX).

in Figs. 4(a) and 4(b). These results were mostly consistent with the PL results and indicated that emission was originated from the iridium complex in the emitting layer. Fig. 5 shows the current density and luminance versus voltage characteristics of the devices with iridium complexes. The maximum luminous efficiencies of device with Ir(ppy)$_2$(ace), Ir(ppy)$_2$(pic), Ir(ppy)$_2$(qc), Ir(F$_2$-ppy)$_2$(pic) and Ir(F$_2$-ppy)$_2$(qc) were 0.88, 13.46, 5.35, 6.54 and 5.50 cd/A, respectively. The Commission Internationale de L'Eclairage (CIE) coordinates of Ir(ppy)$_2$(ace), Ir(ppy)$_2$(pic), Ir(ppy)$_2$(qc) Ir(F$_2$-ppy)$_2$(pic) and Ir(F$_2$-ppy)$_2$(qc) were (0.41, 0.55), (0. 29, 0.60), (0.49, 0.44), (0.15, 0.34) and (0.44, 0.53), respectively.

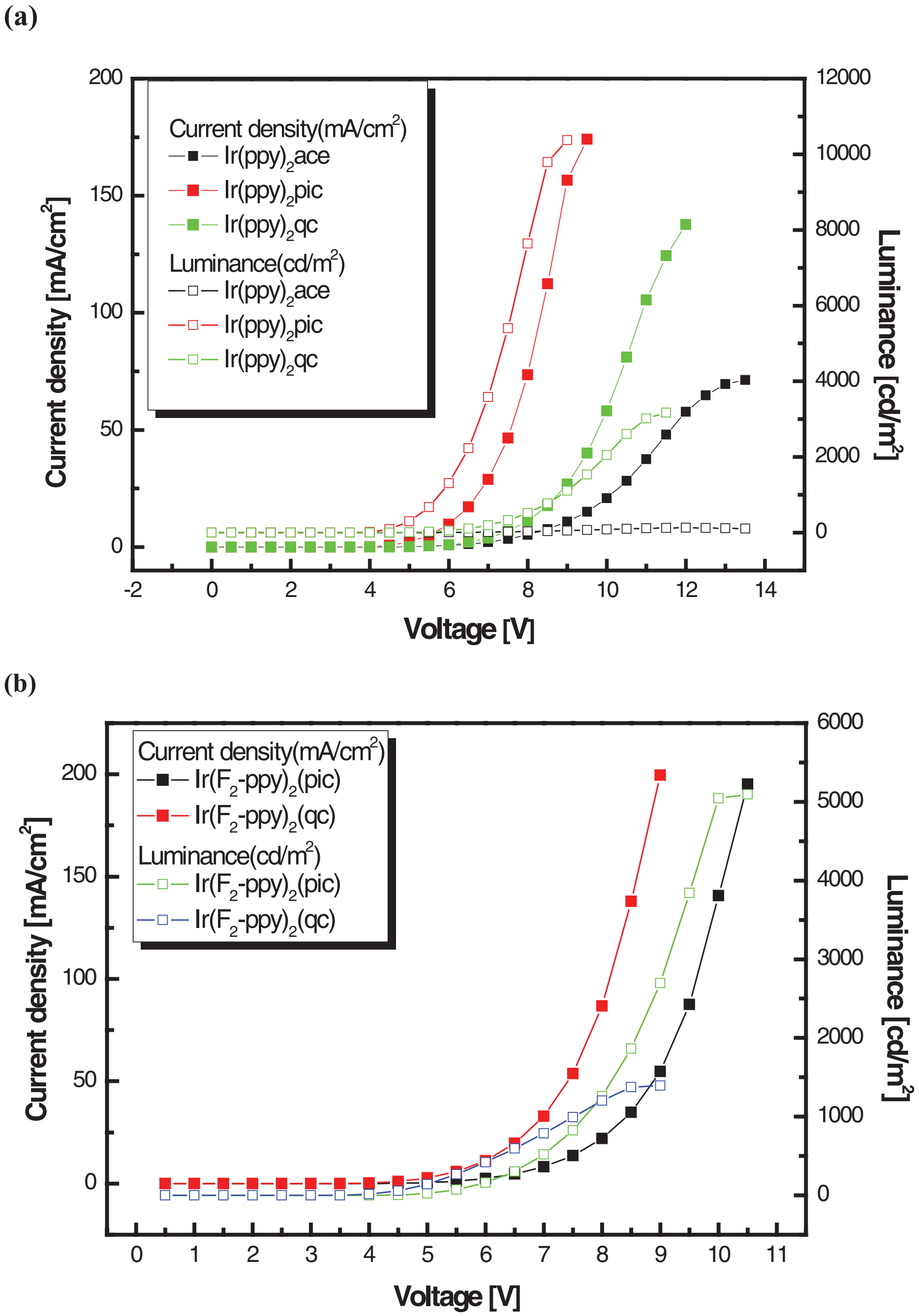

Figure 5. The J-V-L curves of devices containing $Ir(ppy)_2(LX)$ (a) and $Ir(F_2\text{-}ppy)_2(LX)$ (b) in a 10^{-5} M CH_2Cl_2 solution.

Table 2. Characteristics of OLED devices of the iridium complexes

Ir complexes	EL λ_{max} (nm)	Turn-on voltage (V)	Power Efficiency (lm/W)	Quantum Efficiency (%)	Luminance (cd/m^2)	Luminance Efficiency (cd/A)	CIE
Ir(ppy)$_2$(ace)	536	4.5	0.56	0.33	127.3	0.88	(0.41, 0.55)
Ir(ppy)$_2$(pic)	513	5	7.69	4.25	10370	13.46	(0.29, 0.60)
Ir(ppy)$_2$(qc)	592	4	3.06	2.66	3168	5.35	(0.49, 0.44)
Ir(F$_2$-ppy)$_2$(pic)	461	4.5	4.07	3.28	5095	6.54	(0.15, 0.34)
Ir(F$_2$-ppy)$_2$(qc)	559	3.5	3.99	1.92	1395	5.50	(0.44, 0.53)

The device performance of Ir(ppy)$_2$(pic) containing 5-membered ring showed the best result, indicating that 5-membered metallacycle is the most stable in the device. The Ir(ppy)$_2$(pic) showed the best performance in EL because 5-membered metallacycles form the most stable complexes owing to their optimized bond angles. Meanwhile, the Ir(ppy)$_2$(ace) showed the poor device performance presumably due to lack of stability in the 4-membered metallacycle. The overall electroluminescence properties of the iridium complexes were summarized in Table 2.

We also prepared Ir(F$_2$-ppy)$_2$(ace) and tried to fabricate its EL device to compare the luminous efficiencies. However, the attempts to fabricate the EL device containing Ir(F$_2$-ppy)$_2$(ace) as a dopant were failed. The failure of device fabrication could be attributed to the relatively unstable configuration of the 4-membered iridium complex.

Conclusions

We have synthesized and characterized a new series of the iridium complexes bearing acetanilide (ace), picolinate (pic) and 8-quinolinecarboxylate (qc) as ancillary ligands, which can form 4-, 5-, and 6-membered metallacycle with the iridium center, respectively. Considering the UV-Vis, PL and EL patterns of the iridium complexes discussed in this study, we could infer that the various ancillary ligands, ace, pic and qc, lead their iridium complexes to various emission range, from blue to red. Especially, Ir(ppy)$_2$(pic) which has 5-memered ring showed the best EL performance, while Ir(ppy)$_2$(ace) of 4-membered metallacycle showed the poorest performance, reflecting the stability of 5-membered metallacycle compared to that of 4-membered metallacycle.

Acknowledgments

This research was supported by the Korea Research Foundation. (NO. 2011-0003765)

References

[1] Baldo, M. A., O'Brien, D. F., You, Y., Shoustikov, A., Sibley, S., Thompson, M. E., & Forrest, S. R. (1998). *Nature*, *395*, 151.

[2] Lamansky, S., Djurovich, P., Murphy, D., Adbel-Razzaq, F., Lee, H. E., Adachi, C., Burrows, P. E., Forrest, S. R., & Thompson, M. E. (2001). *J. Am. Chem. Soc.*, *123*, 4304.

[3] Ikai, M., Tokito, S., Sakamoto, Y., Suzuki, T., & Taga, Y. (2001). *Appl. Phys. Lett.*, *79*, 156.

[4] Adachi, C., Baldo, M. A., Thompson, M. E., & Forrest, S. R. (2001). *J. Appl. Phys.*, *90*, 5048.

[5] Chen, F. C., Yang, Y., Thompson, M. E., & Kido, J. (2002). *Appl. Phys. Lett.*, *80*, 2308.

[6] Kohler, A., Wilson, J. S., & Friend, R. H. (2002). *Adv. Mater.*, *14*, 701.

[7] Lee, H. S., Ahn, S. Y., Huh, H. S., & Ha, Y. J. (2009). *Organomet. Chem.*, *694*, 3325.

[8] Tsuboyama, A., Iwasaki, H., Furugori, M., Mukaide, T., Kamatani, J., Igawa, T., Moriyama, S., Miura, S., Takiguchi, T., Okada, S., Hoshino, M., & Ueno, K. (2004). *J. Am. Chem. Soc.*, *125*, 12971.

[9] You, Y., Seo, J., Kim, S. H., Kim, K. S., Ahn, T. K., Kim, D., & Park, S. Y. (2008). *Inorg. Chem.*, *47*, 1476.

[10] Thomas, K. R. J., Velusamy, M., Lin, J. T., Chien, C. H., Tao, Y. T., Wen, Y. S., Hu, Y. H., and Chou, P. T. (2005). *Inorg. Chem.*, *44*, 5677.

[11] Yang, C. L., Zhang, X. W., You, H., Zhu, L. Y., Chen, L. Q., Zhu, L. N., Tao, Y. T., Ma, D. G., Shuai, Z. G., & Qin, J. G. (2007). *Adv. Funct. Mater.*, *17*, 651.

[12] You, Y., Kim, K. S., Ahn, T. K., Kim, D., & Park, S. Y. (2007). *J. Phys. Chem. C.*, *111*, 4052.

[13] Shi, M., Li, F., Yi, T., Zhang, D., Hu, H., & Huang, C. (2005). *Inorg. Chem.*, *44*, 8929.

[14] Nazeeruddin, M. K., Humphry-Baker, R., Berner, D., Rivier, S., Zuppiroli, L., & Graetzel, M. (2003). *J. Am. Chem. Soc.*, *125*, 8790.

[15] Park, G. Y., Seo, J. H., Kim, Y. K., Kim, Y. S., & Ha, Y. (2007). *J. Kor. Phys. Soc.*, *50*, 1729.

[16] Yang, W., Fu, H., Song, Q., Zhang, M., & Ding, Y. (2011). *Organometallics.*, *30*, 77.

[17] Nonoyama, M. (1975). *Organomet. Chem.*, *86*, 263.

[18] Kappaun, S., Sax, S., Eder, S., Miller, K. C., Waich, K., Niedermair, F., Saf, R., Mereiter, K., Jacob, J., Mllen, K., List, E. J. W., & Slugovc, C. (2007). *Chem. Mater.*, *19*, 1209.

[19] Minaev, B., Minaeva, V., & Agren, H. (2009). *J. Phys. Chem. A.*, *113*, 726.

[20] Gu, X., Fei, Teng., Zhang, H., Xu, H., Yang, B., Ma, Y., & Liu, X. (2008). *J. Phys. Chem. A.*, *112*, 8387.

[21] Thomas, K. R. J., Velusamy, M., Lin, J. T., Chien, C., Tao, Y., Wen, Y. S., Hu, Y., & Chou, P. (2005). *Inorg. Chem.*, *44*, 5677.

[22] Zhao, Q., Jiang, C., Shi, M., Li, F., Yi, T., Cao, Y., & Huang, C. (2006). *Organnometallics.*, *25*, 3631.